

# Diffusional Enhancement of Autocatalytic Reactions in Catalyst Particles

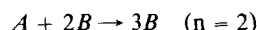
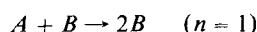
Ajit V. Sapre

Mobil Research and Development Corp.  
Paulsboro Research Laboratory  
Paulsboro, NJ 08066

The problem of simultaneous diffusion and chemical reaction in catalyst particles is well studied for simple power law kinetics and the Langmuir-Hinshelwood type of kinetics. Comprehensive discussions are available in text books by Aris (1975), and by Froment and Bischoff (1979). However, to the best of our knowledge, studies of autocatalytic reactions in catalyst particles are not reported. Such reactions in the presence of solid catalysts, do occur in petroleum and petrochemical processes and also in biochemical systems. Autocatalytic reactions, on the other hand, have been extensively studied in homogeneous CSTRs to analyze phenomena in enzyme systems, combustion, and inorganic solution chemistry, e.g., the oscillatory Belousov-Zhabotinskii reaction. The literature in this area is very rich; the recent articles by Gray and Scott (1983; 1984) give a good overview of this field. In this paper, theoretical aspects of interaction between diffusion and autocatalysis in the isothermal catalyst particles will be presented. Obviously, there are certain similarities between the CSTR and the catalyst particle problem. But important differences remain, which sets the current study separate from the prior work.

## Isothermal Diffusion-Autocatalysis Interaction

The simplest form of autocatalytic reaction may be represented by the prototype reaction steps of the form:

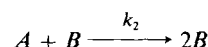
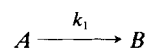


The rate of autocatalytic reaction is given by:

$$\text{rate} \propto C_A C_B^n \quad n = 1, 2$$

We will focus our attention primarily on the quadratic or simple autocatalytic reaction ( $n = 1$ ) and only briefly discuss the cubic autocatalysis ( $n = 2$ ). In the above reaction sequence, reaction will not proceed unless some product species  $[B]$  is initially present. To alleviate this problem of zero initial reaction rate, a par-

allel reaction of the form  $A \rightarrow B$  is added. Thus, the following kinetics represent the reaction sequence studied here.



The behavior of a single isothermal catalyst particle can be represented by the following mass balance. As shown later, very interesting results are obtained without the complexity of non-isothermal behavior.

$$\nabla^2 \underline{De} \underline{C} = \underline{K} \underline{C} \quad (1)$$

For simplicity, effective diffusivity is assumed to be constant and identical for species  $A$  and  $B$ . The above simplifying assumptions retain the interesting features of the problem. Addition of energy balance or variation in diffusivities do not markedly change the character of the problem, and therefore, are left out in this paper. Then, for a slab geometry, Eq. 1 becomes:

$$De \frac{d^2 C_A}{dx^2} = k_1 C_A + k_2 C_A C_B \quad (2)$$

$$C_A + C_B = C_{Ao} + C_{Bo} \quad (3)$$

with boundary conditions,

$$\text{at } X = 0, \quad \frac{dC_A}{dX} = \frac{dC_B}{dX} = 0$$

$$\text{and } X = L, \quad C_A = C_{Ao}; \quad C_B = C_{Bo}$$

Equations 2 and 3 can be nondimensionalized in the following

form:

$$\frac{d^2 X_A}{dZ^2} = \phi_2^2 X_A [\beta^2 + X_B] \quad (4)$$

$$X_B = 1 + \sigma - X_A \quad (5)$$

where

$$Z = X/L$$

$$X_A = C_A/C_{A0}$$

$$X_B = C_B/C_{A0}$$

$$\sigma = C_{B0}/C_{A0}$$

$$\phi_1 = L \sqrt{\frac{k_1}{De}}; \quad \phi_2 = L \sqrt{\frac{k_2 C_{A0}}{De}}; \quad \beta = \frac{\phi_1}{\phi_2}$$

$$L = V_p/S_x$$

As Petersen (1965) showed, both the cylindrical and the spherical particle behavior approaches that for the slab (a mathematically convenient form to solve) when  $V_p/S_x$  is chosen as the length parameter. Solution of Eqs. 4 and 5 in a  $\sigma, \beta$ , and  $\phi_2$  parameter space, completely characterizes this problem. The parameter  $\phi_2$  is defined here as the Thiele modulus for the reaction system. Parameter  $\beta$  defines the relative rate of the first reaction to the second at  $\sigma = 0$ . Parameter  $\sigma$  defines catalyst surface concentrations of  $B$ . The value of  $\beta$  determines the degree of autocatalysis at any  $\sigma$ . For example, when  $\beta$  is small, autocatalysis dominates. As  $\beta$  increases, however, the net conversion of  $A$  can be approximated by simple power law kinetics.

The observed activity of the catalyst particle is given by the usual definition of effectiveness factor ( $\eta$ ):

Effectiveness Factor ( $\eta$ )

$$= \frac{\text{Integral avg. reaction rate of } A \text{ in particle}}{\text{Reaction rate of } A \text{ at surface conditions}} \quad (6)$$

Equations 4 and 5 are solved to determine concentration profiles of  $A$  and  $B$  inside the catalyst particle. Equation 6 is then evaluated to determine the particle effectiveness factor. Equations 4 and 5 were discretized using the orthogonal collocation technique described by Villadsen and Michelsen (1973). The resulting nonlinear set of equations were solved using the Newton-Raphson technique.

## Simulation Results

Equations 4, 5, and 6 were solved for different  $\sigma, \beta$  and  $\phi_2$  values. For example, Figure 1 summarizes the effectiveness factor versus the Thiele modulus curves for  $\beta$  values ranging from 0.022 to 1.0 at  $\sigma = 0$ , i.e., concentration of  $B$  is zero at the surface. For small values of  $\beta$ , significant enhancement in apparent catalyst activity is achieved. Effectiveness factors greater than 400 are obtained at  $\beta = 0.022$ . The effectiveness factors initially increase with increasing Thiele modulus, contrary to the expected effect for an isothermal catalyst particle. The effectiveness factors decrease with increasing Thiele modulus unless

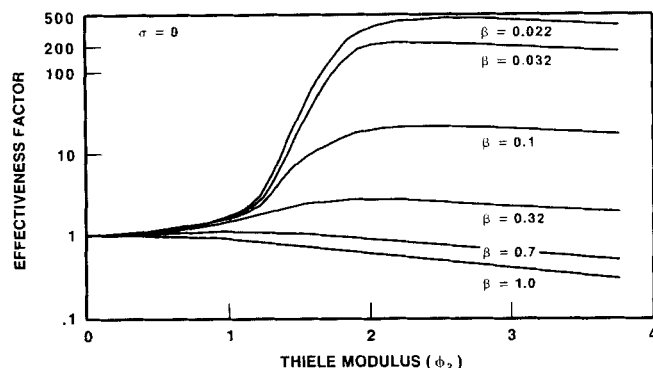


Figure 1. Particle effectiveness factor curves for quadratic autocatalysis.

intraparticle heat transfer effects are dominant for an exothermic reaction. In the present situation, reaction rates are increased due to the presence of rate enhancing species  $[B]$  inside the particle, as a result of the diffusional resistance of the catalyst particle. At very high values of the Thiele modulus, effectiveness factors do decrease due to the ineffective use of catalyst interior, as concentrations of  $[A]$  approach small values. Therefore, with increasing particle size, higher effectiveness factors can be achieved up to a point. Thus, an optimum particle size could be determined for a given set of operating parameters. Figure 1 also shows the effect of  $\beta$  on the effectiveness factors. Effectiveness factors decrease with increasing  $\beta$  at constant  $\phi_2$ . Higher values of  $\beta$  correspond to a larger contribution of  $A \rightarrow B$  reaction to the conversion of  $A$ , and therefore, to the diminishing character of the autocatalytic reaction step. In fact, at  $\beta = 1$  we do not see any diffusional enhancement. The reaction rates of nonautocatalytic and autocatalytic steps are comparable in this case.

Under favorable operating parameters, larger catalyst particles would lead to higher catalyst effectiveness factors for the conversion of  $A$ . Thus, larger particles would allow higher space velocity operation for a flow reactor, reducing the amount and cost of catalyst per unit of  $A$  converted. One could either increase the capacity of a given reactor by increasing catalyst size, or design a smaller reactor for the fixed-capacity. The lower pressure drop with larger particles is a further practical benefit. A specific example for a flow reactor optimization is included here, with the following parameter values:  $k_1 = 0.1 \text{ s}^{-1}$ ,  $k_2 C_{A0} = 10 \text{ s}^{-1}$ , and  $De = 10^{-6} \text{ m}^2/\text{s}$ . A tubular reactor designed to achieve 75% conversion of  $A$  is desired, with the assumption that the concentration of  $B$  is zero at the inlet. The effectiveness factors determined at reactor locations of  $X = 0$  (front), 0.17, 0.33, 0.67, and 1 (end) as a function of particle size are summarized in Figure 2. Several conclusions can be drawn from Figure 2:

- Particle size has pronounced effect on effectiveness factors at the front of a reactor ( $X = 0$ ).
- There is an optimum particle size at each location.
- Effectiveness factors decrease monotonically with increasing particle size towards the exit.

Obviously, it is advantageous to distribute particles of progressively decreasing size along the length of the reactor to achieve optimum performance. The dotted line in Figure 2 shows the optimum particle size distribution.

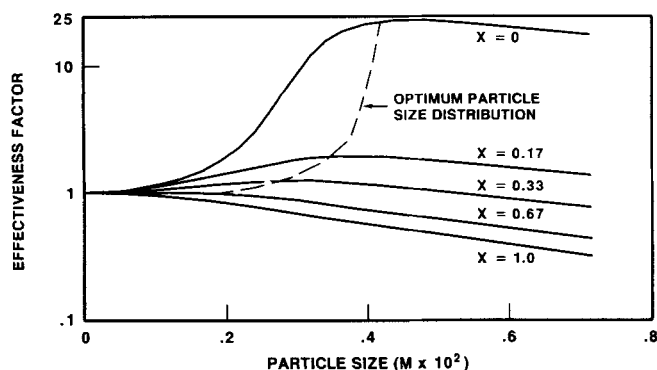


Figure 2. Flow reactor optimization for quadratic autocatalysis.

Lower activity catalysts generally benefit from diffusional enhancement and in such cases, use of larger catalyst size is beneficial. In principle, one could design catalysts (adjust relative rates of the first order and autocatalytic reactions) to achieve maximum effectiveness from the favorable interaction of autocatalysis and particle diffusion phenomenon.

### Cubic Autocatalysis

Analysis of Eqs. 4 and 5 reveals that with quadratic autocatalysis, only one steady state is feasible in the entire parameter space. The cubic autocatalysis on the other hand, can lead to multiplicity, oscillations, and other interesting phenomena. The following nondimensionalized equations describe this reaction sequence with the same boundary conditions as before:

$$\frac{d^2 X_A}{dZ^2} = \phi_2^2 X_A [\beta^2 + X_A^2] \quad (7)$$

$$X_B = 1 + \sigma - X_A \quad (8)$$

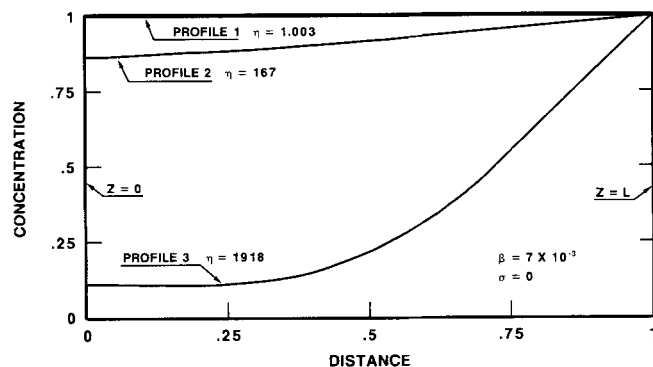


Figure 3. Example of multiplicity for cubic autocatalysis.

where,

$$Z = X/L; \quad X_A = C_A/C_{A0}; \quad X_B = C_B/C_{A0}; \quad \sigma = C_{B0}/C_{A0}$$

$$\phi_1 = L \sqrt{\frac{k_1}{De}}; \quad \phi_2 = L \sqrt{\frac{k_2 C_{A0}^2}{De}}; \quad \beta = \phi_1/\phi_2; \quad L = V_p/S_x$$

A case study showing three steady states is summarized here. For a  $9 \times 10^{-4}$  m diameter catalyst particle, effectiveness factors of 1.003, 167.0, and 1918.0 are feasible for  $k_1 = 0.05 \text{ s}^{-1}$ ,  $k_2 C_{A0} = 100 \text{ s}^{-1}$ , and  $De = 10^{-6} \text{ m}^2/\text{s}$ . The concentration profiles of  $[A]$  for the three steady states are summarized in Figure 3.

It is not surprising that the interaction of autocatalysis and particle diffusion can lead to several interesting phenomena. This system is even richer than the well studied CSTR problem. The lumped CSTR equations represent only a narrow spectrum of the features of the distributed catalyst particle problem.

### Notation

- $A$  = species  $A$
- $B$  = species  $B$
- $C_A$  = concentration of  $A$
- $C_B$  = concentration of  $B$
- $C_{A0}$  = concentration of  $A$  at catalyst surface
- $C_{B0}$  = concentration of  $B$  at catalyst surface
- $De$  = effective diffusion coefficient
- $K$  = matrix of rate constants
- $k_1$  = rate constant, reaction 1
- $k_2$  = rate constant, reaction 2
- $L$  = length scale
- $n$  = order of reaction
- $S_x$  = surface area of catalyst particle
- $V_p$  = volume of catalyst particle
- $X_A$  = concentration of  $A$
- $X$  = particle dimension
- $X_B$  = concentration of  $B$
- $Z$  = distance

### Greek letters

- $\beta$  = Thiele moduli ratio
- $\eta$  = effectiveness factor
- $\sigma$  = surface concentrations ratio
- $\phi_1$  = Thiele modulus, reaction 1
- $\phi_2$  = Thiele modulus, reaction 2

### Literature Cited

- Aris, R., *The Mathematical Theory of Diffusion and Reaction in Permeable Catalysts, I, II*, Oxford University Press, London (1975).
- Froment, G. F., and K. B. Bischoff, *Chemical Reactor Analysis and Design*, John Wiley, New York (1979).
- Gray, P., and S. K. Scott, "Autocatalytic Reactions in the Isothermal Continuous Stirred Tank Reactor: Oscillations and Instabilities," *Chem. Eng. Sci.*, **39**(6), 1087 (1984).
- Gray, P., and S. K. Scott, "Autocatalytic Reactions in the Isothermal Continuous Stirred Tank Reactor: Isola and Other Forms of Multiplicity," *Chem. Eng. Sci.*, **38**(1), 29 (1983).
- Petersen, E. E., *Chemical Reaction Analysis*, Prentice Hall, New York (1965).
- Villadsen, J., and M. I. Michelsen, *Solution of Differential Equation Models by Polynomial Approximation*, Prentice Hall (1973).

Manuscript received Aug. 22, 1988, and revision received Nov. 7, 1988.